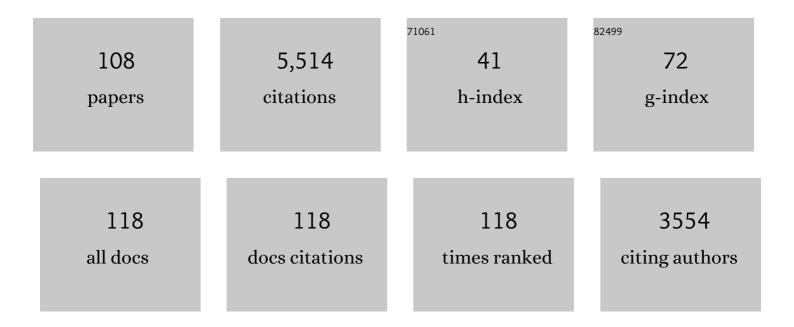
## Anne Mangeney

List of Publications by Year in descending order

Source: https://exaly.com/author-pdf/3926634/publications.pdf Version: 2024-02-01



#	Article	IF	CITATIONS
1	Simplified simulation of rock avalanches and subsequent debris flows with a single thin-layer model: Application to the Prêcheur river (Martinique, Lesser Antilles). Engineering Geology, 2022, 296, 106457.	2.9	7
2	A bed pressure correction of the friction term for depth-averaged granular flow models. Applied Mathematical Modelling, 2022, 106, 627-658.	2.2	2
3	Dilatancy in dry granular flows with a compressible μ(I) rheology. Journal of Computational Physics, 2021, 429, 110013.	1.9	8
4	A Weakly Non-hydrostatic Shallow Model for Dry Granular Flows. Journal of Scientific Computing, 2021, 86, 1.	1.1	11
5	Explicit solutions to a free interface model for the static/flowing transition in thin granular flows. ESAIM: Mathematical Modelling and Numerical Analysis, 2021, 55, S369-S395.	0.8	4
6	Seismology and Environment. Encyclopedia of Earth Sciences Series, 2021, , 1655-1661.	0.1	0
7	Some analytical solutions for validation of free surface flow computational codes. Journal of Fluid Mechanics, 2021, 913, .	1.4	2
8	Assessing the effect of lithological setting, block characteristics and slope topography on the runout length of rockfalls in the Alps and on the island of La Réunion. Natural Hazards and Earth System Sciences, 2021, 21, 1159-1177.	1.5	4
9	Locating Rockfalls Using Inter‣tation Ratios of Seismic Energy at Dolomieu Crater, Piton de la Fournaise Volcano. Journal of Geophysical Research F: Earth Surface, 2021, 126, e2020JF005715.	1.0	6
10	Experimental assessment of the effective friction at the base of granular chute flows on a smooth incline. Physical Review E, 2021, 103, 042905.	0.8	13
11	Topography Curvature Effects in Thinâ€Layer Models for Gravityâ€Driven Flows Without Bed Erosion. Journal of Geophysical Research F: Earth Surface, 2021, 126, e2020JF005657.	1.0	13
12	Laboratory Landquakes: Insights From Experiments Into the Highâ€Frequency Seismic Signal Generated by Geophysical Granular Flows. Journal of Geophysical Research F: Earth Surface, 2021, 126, e2021JF006172.	1.0	8
13	Dynamics of recent landslides (<20 My) on Mars: Insights from high-resolution topography on Earth and Mars and numerical modelling. Planetary and Space Science, 2021, 206, 105303.	0.9	10
14	Synthetic benchmarking of concentrated pyroclastic current models. Bulletin of Volcanology, 2021, 83, 1.	1.1	12
15	A two-layer shallow flow model with two axes of integration, well-balanced discretization and application to submarine avalanches. Journal of Computational Physics, 2020, 406, 109186.	1.9	8
16	Triggering granular avalanches with ultrasound. Physical Review E, 2020, 102, 042901.	0.8	11
17	Simulation of Topography Effects on Rockfallâ€Generated Seismic Signals: Application to Piton de la Fournaise Volcano. Journal of Geophysical Research: Solid Earth, 2020, 125, e2020JB019874.	1.4	6
18	Operational Estimation of Landslide Runout: Comparison of Empirical and Numerical Methods. Geosciences (Switzerland), 2020, 10, 424.	1.0	11

ANNE MANGENEY

#	Article	IF	CITATIONS
19	Modelling capsizing icebergs in the open ocean. Geophysical Journal International, 2020, 223, 1265-1287.	1.0	5
20	Analysis of the 2017 June Maoxian landslide processes with force histories from seismological inversion and terrain features. Geophysical Journal International, 2020, 222, 1965-1976.	1.0	8
21	Multilayer models for shallow two-phase debris flows with dilatancy effects. Journal of Computational Physics, 2020, 419, 109699.	1.9	7
22	Constraining landslide characteristics with Bayesian inversion of field and seismic data. Geophysical Journal International, 2020, 221, 1341-1348.	1.0	18
23	Seismology and Environment. Encyclopedia of Earth Sciences Series, 2020, , 1-8.	0.1	1
24	Relations Between the Characteristics of Granular Column Collapses and Resultant Highâ€Frequency Seismic Signals. Journal of Geophysical Research F: Earth Surface, 2019, 124, 2987-3021.	1.0	16
25	Modeling of partial dome collapse of La Soufrière of Guadeloupe volcano: implications for hazard assessment and monitoring. Scientific Reports, 2019, 9, 13105.	1.6	31
26	Monitoring Greenland ice sheet buoyancy-driven calving discharge using glacial earthquakes. Annals of Glaciology, 2019, 60, 75-95.	2.8	17
27	Empirical investigation of friction weakening of terrestrial and Martian landslides using discrete element models. Landslides, 2019, 16, 1121-1140.	2.7	21
28	Numerical approximation of the 3D hydrostatic Navier–Stokes system with free surface. ESAIM: Mathematical Modelling and Numerical Analysis, 2019, 53, 1981-2024.	0.8	3
29	Elastic wave generated by granular impact on rough and erodible surfaces. Journal of Applied Physics, 2018, 123, 044901.	1.1	18
30	Forensic investigations of the Cima Salti Landslide, northern Italy, using runout simulations. Geomorphology, 2018, 318, 172-186.	1.1	5
31	2D granular flows with the μ(I) rheology and side walls friction: A well-balanced multilayer discretization. Journal of Computational Physics, 2018, 356, 192-219.	1.9	38
32	On the Link Between External Forcings and Slope Instabilities in the Piton de la Fournaise Summit Crater, Reunion Island. Journal of Geophysical Research F: Earth Surface, 2018, 123, 2422-2442.	1.0	23
33	Numerical Modeling of Iceberg Capsizing Responsible for Glacial Earthquakes. Journal of Geophysical Research F: Earth Surface, 2018, 123, 3013-3033.	1.0	7
34	Estimation of dynamic friction and movement history of large landslides. Landslides, 2018, 15, 1963-1974.	2.7	34
35	Link Between the Dynamics of Granular Flows and the Generated Seismic Signal: Insights From Laboratory Experiments. Journal of Geophysical Research F: Earth Surface, 2018, 123, 1407-1429.	1.0	23
36	Continuum viscoplastic simulation of a granular column collapse on large slopes: <i>μ</i> ( <i>I</i> ) rheology and lateral wall effects. Physics of Fluids, 2017, 29, .	1.6	52

#	Article	IF	CITATIONS
37	Two-dimensional simulation by regularization of free surface viscoplastic flows with Drucker–Prager yield stress and application to granular collapse. Journal of Computational Physics, 2017, 333, 387-408.	1.9	14
38	Spatio-temporal evolution of rockfall activity from 2007 to 2011 at the Piton de la Fournaise volcano inferred from seismic data. Journal of Volcanology and Geothermal Research, 2017, 333-334, 36-52.	0.8	27
39	Numerical simulation of the 30–45Âka debris avalanche flow of Montagne Pelée volcano, Martinique: from volcano flank collapse to submarine emplacement. Natural Hazards, 2017, 87, 1189-1222.	1.6	31
40	The dynamic response of prone-to-fall columns to ambient vibrations: comparison between measurements and numerical modelling. Geophysical Journal International, 2017, 208, 1058-1076.	1.0	33
41	Granular and particle-laden flows: from laboratory experiments to field observations. Journal Physics D: Applied Physics, 2017, 50, 053001.	1.3	146
42	A Free Interface Model for Static/Flowing Dynamics in Thin-Layer Flows of Granular Materials with Yield: Simple Shear Simulations and Comparison with Experiments. Applied Sciences (Switzerland), 2017, 7, 386.	1.3	10
43	A two-phase solid-fluid model for dense granular flows including dilatancy effects: comparison with submarine granular collapse experiments. EPJ Web of Conferences, 2017, 140, 09039.	0.1	15
44	Application of a Combined Finite Element—Finite Volume Method to a 2D Non-hydrostatic Shallow Water Problem. Springer Proceedings in Mathematics and Statistics, 2017, , 219-226.	0.1	1
45	Complex force history of a calvingâ€generated glacial earthquake derived from broadband seismic inversion. Geophysical Research Letters, 2016, 43, 1055-1065.	1.5	24
46	A multilayer shallow model for dry granular flows with the -rheology: application to granular collapse on erodible beds. Journal of Fluid Mechanics, 2016, 798, 643-681.	1.4	41
47	A two-phase two-layer model for fluidized granular flows with dilatancy effects. Journal of Fluid Mechanics, 2016, 801, 166-221.	1.4	67
48	Resolving source mechanisms of microseismic swarms induced by solution mining. Geophysical Journal International, 2016, 206, 696-715.	1.0	12
49	Estimation of dynamic friction of the Akatani landslide from seismic waveform inversion and numerical simulation. Geophysical Journal International, 2016, 206, 1479-1486.	1.0	34
50	Experimental validation of theoretical methods to estimate the energy radiated by elastic waves during an impact. Journal of Sound and Vibration, 2016, 362, 176-202.	2.1	22
51	An analytic approach for the evolution of the static/flowing interface in viscoplastic granular flows. Communications in Mathematical Sciences, 2016, 14, 2101-2126.	0.5	17
52	On the shaping factors of the secondary microseismic wavefield. Journal of Geophysical Research: Solid Earth, 2015, 120, 6241-6262.	1.4	53
53	Numerical modeling of the Mount Meager landslide constrained by its force history derived from seismic data. Journal of Geophysical Research: Solid Earth, 2015, 120, 2579-2599.	1.4	71
54	A two-phase shallow debris flow model with energy balance. ESAIM: Mathematical Modelling and Numerical Analysis, 2015, 49, 101-140.	0.8	46

ANNE MANGENEY

#	Article	IF	CITATIONS
55	Friction weakening in granular flows deduced from seismic records at the Soufrière Hills Volcano, Montserrat. Journal of Geophysical Research: Solid Earth, 2015, 120, 7536-7557.	1.4	59
56	Characterization of rockfalls from seismic signal: Insights from laboratory experiments. Journal of Geophysical Research: Solid Earth, 2015, 120, 7102-7137.	1.4	41
57	Toward continuous quantification of lava extrusion rate: Results from the multidisciplinary analysis of the 2 January 2010 eruption of Piton de la Fournaise volcano, La Réunion. Journal of Geophysical Research: Solid Earth, 2015, 120, 3026-3047.	1.4	23
58	Location of microseismic swarms induced by salt solution mining. Geophysical Journal International, 2015, 200, 337-362.	1.0	22
59	Viscoplastic modeling of granular column collapse with pressure-dependent rheology. Journal of Non-Newtonian Fluid Mechanics, 2015, 219, 1-18.	1.0	116
60	Model Space Exploration for Determining Landslide Source History from Long-Period Seismic Data. Pure and Applied Geophysics, 2015, 172, 389-413.	0.8	29
61	An energy-consistent depth-averaged Euler system: Derivation and properties. Discrete and Continuous Dynamical Systems - Series B, 2015, 20, 961-988.	0.5	32
62	Frictional velocity-weakening in landslides on Earth and on other planetary bodies. Nature Communications, 2014, 5, 3417.	5.8	224
63	An Automatic Kurtosis-Based P- and S-Phase Picker Designed for Local Seismic Networks. Bulletin of the Seismological Society of America, 2014, 104, 394-409.	1.1	171
64	Automated identification, location, and volume estimation of rockfalls at Piton de la Fournaise volcano. Journal of Geophysical Research F: Earth Surface, 2014, 119, 1082-1105.	1.0	94
65	Fundamental changes of granular flow dynamics, deposition, and erosion processes at high slope angles: Insights from laboratory experiments. Journal of Geophysical Research F: Earth Surface, 2014, 119, 504-532.	1.0	100
66	Highâ€resolution bathymetry reveals contrasting landslide activity shaping the walls of the Midâ€Atlantic Ridge axial valley. Geochemistry, Geophysics, Geosystems, 2013, 14, 996-1011.	1.0	37
67	Exact solution for granular flows. International Journal for Numerical and Analytical Methods in Geomechanics, 2013, 37, 1408-1433.	1.7	76
68	Modelling secondary microseismic noise by normal mode summation. Geophysical Journal International, 2013, 193, 1732-1745.	1.0	86
69	Dynamic pore-pressure variations induce substrate erosion by pyroclastic flows. Geology, 2013, 41, 1107-1110.	2.0	58
70	Modelling long-term seismic noise in various environments. Geophysical Journal International, 2012, 191, 707-722.	1.0	104
71	Numerical modeling of the Mount Steller landslide flow history and of the generated long period seismic waves. Geophysical Research Letters, 2012, 39, .	1.5	108
72	LiDAR derived morphology of the 1993 Lascar pyroclastic flow deposits, and implication for flow dynamics and rheology. Journal of Volcanology and Geothermal Research, 2012, 245-246, 81-97.	0.8	36

Anne Mangeney

#	Article	IF	CITATIONS
73	Ocean wave sources of seismic noise. Journal of Geophysical Research, 2011, 116, .	3.3	246
74	Influence of the scar geometry on landslide dynamics and deposits: Application to Martian landslides. Journal of Geophysical Research, 2011, 116, .	3.3	46
75	Slope instabilities in Dolomieu crater, Réunion Island: From seismic signals to rockfall characteristics. Journal of Geophysical Research, 2011, 116, .	3.3	137
76	On the run-out distance of geophysical gravitational flows: Insight from fluidized granular collapse experiments. Earth and Planetary Science Letters, 2011, 311, 375-385.	1.8	65
77	Landslide boost from entrainment. Nature Geoscience, 2011, 4, 77-78.	5.4	46
78	A Riemann solver for single-phase and two-phase shallow flow models based on relaxation. Relations with Roe and VFRoe solvers. Journal of Computational Physics, 2011, 230, 515-550.	1.9	26
79	Sinuous gullies on Mars: Frequency, distribution, and implications for flow properties. Journal of Geophysical Research, 2010, 115, .	3.3	118
80	Numerical modeling of landquakes. Geophysical Research Letters, 2010, 37, .	1.5	110
81	Erosion and mobility in granular collapse over sloping beds. Journal of Geophysical Research, 2010, 115, .	3.3	200
82	Simulation of Tsaoling landslide, Taiwan, based on Saint Venant equations over general topography. Engineering Geology, 2009, 104, 181-189.	2.9	79
83	Results of Back-Analysis of the Propagation of Rock Avalanches as a Function of the Assumed Rheology. Rock Mechanics and Rock Engineering, 2008, 41, 59-84.	2.6	117
84	On new erosion models of Savage–Hutter type for avalanches. Acta Mechanica, 2008, 199, 181-208.	1.1	87
85	A new Savage–Hutter type model for submarine avalanches and generated tsunami. Journal of Computational Physics, 2008, 227, 7720-7754.	1.9	136
86	A Roe-type scheme for two-phase shallow granular flows over variable topography. ESAIM: Mathematical Modelling and Numerical Analysis, 2008, 42, 851-885.	0.8	111
87	High Order Finite Volume Methods Applied to Sediment Transport and Submarine Avalanches. , 2008, , 247-258.		2
88	Numerical Modeling of Two-Phase Gravitational Granular Flows with Bottom Topography. , 2008, , 825-832.		7
89	Numerical modeling of self-channeling granular flows and of their levee-channel deposits. Journal of Geophysical Research, 2007, 112, .	3.3	145
90	Mobility and topographic effects for large Valles Marineris landslides on Mars. Geophysical Research Letters, 2007, 34, .	1.5	75

Anne Mangeney

#	Article	IF	CITATIONS
91	Avalanche mobility induced by the presence of an erodible bed and associated entrainment. Geophysical Research Letters, 2007, 34, .	1.5	113
92	The effect of the earth pressure coefficients on the runout of granular material. Environmental Modelling and Software, 2007, 22, 1437-1454.	1.9	71
93	Memory of the unjamming transition during cyclic tiltings of a granular pile. Physical Review E, 2005, 72, 051305.	0.8	28
94	On the use of Saint Venant equations to simulate the spreading of a granular mass. Journal of Geophysical Research, 2005, 110, .	3.3	161
95	Spreading of a granular mass on a horizontal plane. Physics of Fluids, 2004, 16, 2371-2381.	1.6	279
96	A new model of Saint Venant and Savage–Hutter type for gravity driven shallow water flows. Comptes Rendus Mathematique, 2003, 336, 531-536.	0.1	121
97	Mesh size selection in a soil-biosphere-atmosphere transfer model. Journal of Environmental Engineering and Science, 2003, 2, 77-81.	0.3	1
98	Short Note: Precision and Convergence of a Steady Two-Dimensional Ice Sheet Flow Model. Mathematical Geosciences, 2001, 33, 229-237.	0.9	0
99	Analytical Solution for Testing Debris Avalanche Numerical Models. Pure and Applied Geophysics, 2000, 157, 1081-1096.	0.8	118
100	Modeling of debris avalanche and generated water waves: Application to real and potential events in Montserrat. Physics and Chemistry of the Earth, 2000, 25, 741-745.	0.6	26
101	Numerical modeling of a landslide-generated tsunami following a potential explosion of the Montserrat volcano. Physics and Chemistry of the Earth, 1999, 24, 163-168.	0.6	25
102	Anisotropic behavior of GRIP ices and flow in Central Greenland. Earth and Planetary Science Letters, 1998, 154, 307-322.	1.8	51
103	The shallow ice approximation for anisotropic ice: Formulation and limits. Journal of Geophysical Research, 1998, 103, 691-705.	3.3	31
104	Simulation of water waves generated by a potential debris avalanche in Montserrat, Lesser Antilles. Geophysical Research Letters, 1998, 25, 3697-3700.	1.5	52
105	A numerical study of anisotropic, low Reynolds number, free surface flow for ice sheet modeling. Journal of Geophysical Research, 1997, 102, 22749-22764.	3.3	43
106	Isothermal flow of an anisotropic ice sheet in the vicinity of an ice divide. Journal of Geophysical Research, 1996, 101, 28189-28204.	3.3	41
107	Greenland under changing climates: sensitivity experiments with a new three-dimensional ice-sheet model. Annals of Glaciology, 1995, 21, 1-7.	2.8	48
108	A two-dimensional method for a family of dispersive shallow water models. SMAI Journal of Computational Mathematics, 0, 6, 187-226.	0.0	6